Differential heterodyne detection with diffractive optics for multidimensional transient-grating spectroscopy

Champak Khurmi and Mark A. Berg*

Department of Chemistry and Biochemistry, University of South Carolina, Columbia, South Carolina 29208, USA
**Corresponding author: berg@mail.chem.sc.edu*

Received September 10, 2009; accepted October 9, 2009;
posted October 14, 2009 (Doc. ID 116995); published November 18, 2009

Heterodyne detection with a local oscillator generated by a diffractive optic provides good phase stability, but suffers from interfering single-beam-bleach signals. This interference is a problem in four-beam transient gratings, but becomes more severe in higher order transient gratings. A simple and low noise method to eliminate this interference is demonstrated in both a four-wave-mixing, first-order–transient-grating experiment and in a six-wave-mixing, second-order–transient-grating experiment.
OCIS codes: 300.6310, 300.6500, 320.7150, 050.1970.

1. INTRODUCTION

Heterodyne detection of optical signals has become common in time-resolved nonlinear spectroscopy because it has several major advantages: it increases absolute signal sizes, it separates real and imaginary contributions to the signal, and it gives a signal linear in the population, as opposed to the quadratic signal given by homodyne detection. Diffractive-optics methods, introduced by Maznev *et al.* [1] and Goodno *et al.* [2,3] in the context of transient-grating experiments, make it much easier to meet the phase-stability requirements of heterodyne detection. However, the straightforward application of these methods has the local oscillator passing through the excited region of the sample. The resulting single-beam-bleach signals can be a significant problem [4–7].

We have recently introduced what we believe to be a new time-resolved spectroscopy called multiple population-period transient spectroscopy (MUPPETS) that uses six-wave mixing to discriminate between heterogeneous and homogeneous causes of nonexponential decay [8–12]. MUPPETS can be regarded as the extension of transient-grating spectroscopy to higher order: more than one pair of excitation pulses create the final grating. Second-order MUPPETS, which uses two pairs of excitation pulses, has already been demonstrated experimentally [8–10]. Theoretical work suggests that third-order MUPPETS, a type of nine-wave mixing, will also be useful [11,12]. These high-order spectroscopies have smaller signals than four-wave-mixing experiments and have correspondingly stricter demands for eliminating interfering signals and reducing noise.

In this paper, we propose and test what we believe to be a new method of heterodyne detection for transient gratings, both standard and high order. We detect the difference in signals from detectors placed in each of the beams that are conventionally regarded as the probe and local oscillator, although in our configuration, the distinction between these beams disappears. This differential-detection method suppresses the single-beam-bleach signals that occur when using diffractive optics. Major reductions in noise result from eliminating the need to subtract this large background from the measurements. Additional noise reduction comes from cancellation of pulse-to-pulse fluctuations in the laser power.

Several methods for eliminating the single-beam bleach have already been suggested. Xu *et al.* [5] chopped the probe beam rather than one of the pump beams, so the single-beam-bleach interference became a delay-independent background. Nonetheless, this large background still contributes to noise in the measurement. Khalil *et al.* [4] discarded the original local oscillator and used a second diffractive optic after the sample to regenerate it. Kubarych *et al.* showed that the local oscillator can be temporally displaced before the excitation pulses, if spectral interferometry is used in the detection [6]. Ammend and Blank [7] spatially displaced the local oscillator beam so it did not pass through the excited region of the sample and then recombined it with the signal using additional optics after the sample. These latter methods increase the experimental complexity and spectral interferometry can limit the range of delays used. Our method only requires adding a second detector to a standard system. The single-beam bleach can also be avoided by dropping the use of diffractive optics, but then the advantages of passive phase stabilization and automatic phase matching are also lost.

Ogilvie *et al.* [13] have demonstrated a two-detector method similar to the one reported here. However, in their report, the method was limited to detecting the real part of the susceptibility, and the theory was only developed for first-order gratings. Our generalization of this idea allows both parts of the susceptibility to be measured, and the theory is extended to any order grating.

Our method can be compared with balanced-detection

methods used with an external local oscillator [14–16]. In those methods, the two detected beams are generated when the external local oscillator is combined with the signal on a beam splitter. The phase is shifted 180° between the two beams, so subtracting the two signals eliminates phase-independent signals. This approach does not transfer to a diffractive-optics setup in a simple way. Our method achieves a similar result with a diffractive-optics local oscillator, although the method of creating the phase shift differs.

2. EXPERIMENTAL METHODS

The optical setup is shown in Fig. 1. This apparatus is also described in our previous papers [8–10]. Pulses at 400 nm were generated by frequency doubling the 800 nm, 50 fs pulse produced from a 1 kHz Ti:sapphire regenerative amplifier system. Transmission gratings that produce three nearly equal intensity diffracted beams (−1, 0, +1 order) were used. Nine beams were created from one input beam by using two transmission gratings (G1 and G2) oriented with their grooves perpendicular to each other. A set of phase-matched beams for either first- or second-order transient gratings were selected by mask M1. Delay lines were placed before G2, so that both beams of each grating pair were scanned simultaneously. The region between grating G2 and the sample was covered to keep the phase of each pair of beams stable. In the second-order experiment, beams occur at different distances from the centers of the lenses giving rise to spherical aberration. The positions of the meniscus lens (L6 and L8) were adjusted to correct this aberration. Auramine in methanol (~0.3 mM, OD 0.45 at 400 nm), a system we have studied before [8,9], was used as the sample. At the sample, the pulse width was 200 fs due to dispersion in the optics, and the energy of each pulse was 200 nJ.

To implement differential detection, unamplified photodiodes with matched RC circuits were placed in each probe beam, and the signals were fed into the differential inputs of a lock-in amplifier. Beam 1a was synchronously chopped so as to block alternate laser pulses (500 Hz modulation). A neutral density filter (ND=1) was placed in one of the probe beams to give the conditions needed to detect both real and imaginary components of the susceptibility [Eq. (14)]. To match the time delay between the probe beams, another filter (ND=0) of the same thickness was placed in the other probe beam. The phase of the detection was changed by adjusting the angle of this filter slightly. All signals are normalized to the intensity measured on the detector when the excitation beams are blocked and the probe beam is chopped and detected at 1 kHz. To collect the appropriate difference signal, a variable neutral density filter was placed in the stronger probe beam and adjusted to give a zero differential signal when the excitation beams were blocked. This procedure is equivalent to taking the difference of normalized signals [Eq. (7)].

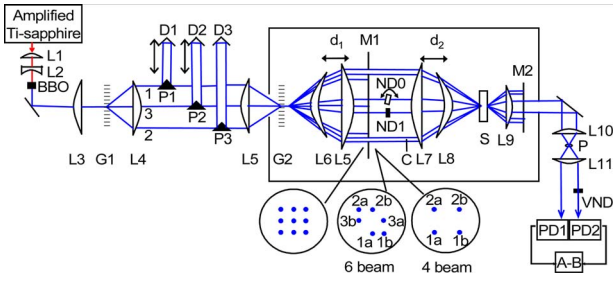

Fig. 1. (Color online) Schematic of the optical setup: L1–L11, lenses; G1 and G2, transmission gratings; P1–P3, reflective prisms; D1–D3, delay lines; C, chopper; ND0 and ND1, neutral density filters; S, sample; M1 and M2, masks; P, pinhole; PD1 and PD2, matched photodiodes; VND, linear variable neutral density filter; A-B, differential inputs of a lock-in amplifier. Different masks are used for the four-beam, first-order grating and for the six-beam, second-order grating as shown.

3. THEORY AND EXPERIMENTAL RESULTS

A. Creation and Detection of Gratings of Arbitrary Order

We begin by considering the creation of a grating of arbitrary order. The excitation consists of N excitations, $n=1,\ldots,N$, each of which is created by a pair of pulses, $j=a,b$. Assuming short pulses, the electric fields can be written as

$$\mathcal{E}_{nj}(t,\mathbf{r}) = E_{nj}\delta(t - t_n + \mathbf{k}_{nj}\cdot\mathbf{r})e^{-i(\mathbf{k}_{nj}\cdot\mathbf{r}+\varphi_{nj}+\omega_n t)}. \quad (1)$$

The pulses are assumed to be transform limited, and the phases φ_{nj} are set so that the electric-field amplitudes E_{nj} are real. Both pulses in a pair have the same frequency ω_n and arrival time t_n, but each pulse has its own phase φ_{nj} and k vector $\mathbf{k}_{nj}$. These fields act on a ground-state solute with a number density ρ to create a change in the ground-state density

$$\delta\rho = \rho\sum_{n=1}^{N}\left[\prod_{m=1}^{n}(-\sigma_m)(I_{ma} + \mathcal{E}_{ma}\mathcal{E}_{mb}^{*} + \mathcal{E}_{ma}^{*}\mathcal{E}_{mb} + I_{mb})\right] \times C^{(n)}(\tau_n,\ldots,\tau_1). \quad (2)$$

The total fluence of the beams, $I_{mj}=E_{mj}^2$ (in photon/cm^2), has been introduced by absorbing the associated constants into the cross section for creating each grating σ_m. The density change decays with an nth-order correlation function $C^{(n)}$, which depends on n time intervals, $\tau_n = t_{n+1}-t_n$. For simplicity, this time dependence will not be displayed hereafter. The first and last terms in parentheses in Eq. (2) represent spatially uniform bleaches due to a single excitation beam; the second and third terms are true mth-order gratings created by pairs of pulses. More detailed discussions of the correlation functions, ground-state versus excited-state gratings, and the appropriate values of the cross sections are found in our other papers [11,12].

These gratings are probed by two pulses designated by $n=N+1$ and $j=a,b$. These pulses are conventionally described as probe (a) and local oscillator (b), but in the setup used here, where both pulses pass through the sample and both pulses are detected, there is no *a priori* distinction between them. These pulses create a nonlinear polarization

$$\mathcal{P} = \chi\delta\rho(\mathcal{E}_{N+1,a} + \mathcal{E}_{N+1,b} + \text{c.c.}). \quad (3)$$

Whereas the cross sections only contain contributions from ground-state absorption and excited-state emission,

the molecular linear susceptibility χ also contains contributions from excited-state absorption and from the index of refraction [12].

We assume that the probe beams are arranged to phase match the desired Nth-order grating

$$\sum_{n=1}^{N+1} \mathbf{k}_{nb} - \mathbf{k}_{na} = 0, \tag{4}$$

but to not phase match any of the other gratings created in the sample. However, the single-beam-bleach terms are always phase matched and cannot be eliminated in any phase-matching pattern. The resulting polarization envelope in the direction of the b-probe beam is

$$P_{N+1,b} = \rho\chi e^{-i\varphi_{N+1,b}}\left[-E_{N+1,b}\sum_{nj} \sigma_n I_{nj} C^{(1)} + (-1)^N e^{i\Phi} E_{N+1,a}\left(\prod_{n=1}^{N} \sigma_n E_{na} E_{nb}\right) C^{(N)}\right], \tag{5}$$

where the total phase of the Nth-order grating is

$$\Phi = \sum_{n=1}^{N+1} \varphi_{nb} - \varphi_{na}. \tag{6}$$

The first term in Eq. (5) represents the single-beam bleaches; the second term is the grating. Other interactions of the local oscillator with the excited sample are smaller, higher order terms. The single-beam bleach is a special problem because it is as large or larger than the desired signal.

B. Standard Detection

The standard method for detecting the grating is to put a single detector in the b-probe beam, chop one of the pump beams, and measure the modulated signal. Here beam $1a$ is taken as the chopped beam for specificity leading to a normalized signal

$$S_b[1a] = \frac{I_{N+1,b}(I_{1a}) - I_{N+1,b}(I_{1a}=0)}{2I_{N+1,b}(I_{1a}=0)} \approx -\frac{4\pi\omega L}{cI_{N+1,b}} \mathrm{Im}\, E_{N+1,b} e^{i\varphi_{N+1,b}} P_{N+1,b}. \tag{7}$$

(Square brackets are used to denote signal processing conditions rather than functional dependence.) In the second equation, we have neglected weak homodyne terms. The length of the sample is L. Using the polarization in Eq. (5) gives the single-detector signal,

$$S_b^{(N)}[1a] = \frac{4\pi\omega L\rho}{c}\left[(\mathrm{Im}\ \chi)\sigma_1 I_1 C^{(1)} + (-1)^{N-1}\ \mathrm{Im}(\chi e^{i\Phi}) \sqrt{\frac{I_{N+1,a}}{I_{N+1,b}}}\left(\prod_{n=1}^{N} \sigma_n I_n\right) C^{(N)}\right]. \tag{8}$$

As expected, the phase of the experiment Φ can be varied to measure different components of the susceptibility in the Nth-order grating, but the single-beam bleach depends only on the absorptive component of the susceptibility and is independent of phase. The component of the grating measured can be selected by manipulating the phase of any beam in the experiment [Eq. (6)].

In the case of a first-order grating, the sizes of the single-beam bleach and the grating are approximately equal. In addition, the correlation function for each term is the same for $N=1$, so the consequences of not completely separating these terms are not great. However, for a higher order grating, these consequences are more severe. Contamination of a multiple-time correlation function with the single-time correlation function would lead to a misinterpretation of the results. Moreover, because the saturation of the transition is typically small, $\sigma_n I_n \leq 0.1$, the single-beam interference will be much stronger than the desired grating signal.

A common way to discriminate between these terms is to use their differing phase dependence by adding or subtracting two scans whose phase differs by 180°,

$$S_b[1a,\Phi\pm] = \tfrac{1}{2}[S_b[1a](\Phi_0) \pm S_b[1a](\Phi_0+\pi)]. \tag{9}$$

The addition yields the single-beam bleach (as well as various other interfering signals not explicitly considered here). The subtraction isolates the grating term,

$$S_b^{(N)}[1a,\Phi-] = (-1)^{N-1}\frac{4\pi\omega L\rho}{c}(\chi''\cos\Phi + \chi'\sin\Phi)\sqrt{\frac{I_{N+1,a}}{I_{N+1,b}}}\left(\prod_{n=1}^{N+1}\sigma_n I_n\right) C^{(N)}. \tag{10}$$

These ideas are illustrated in Fig. 2. Figure 2(A) shows the in-phase (Φ_0) and out-of-phase ($\Phi_0+\pi$) signals for a first-order grating determined by the maximum and minimum signal strengths. The signals are very asymmetric, being a combination of grating and single-beam-bleach signals. These terms are separated in Fig. 2(C) by addition and subtraction of the traces. The grating and single-beam bleach have similar amplitudes and decay profiles.

Figures 2(B) and 2(D) show similar measurements for a second-order grating. Now the grating signal is much smaller than the single-beam bleach. Reversing the phase causes only a small change in the signal [Fig. 2(B)]. Adding and subtracting in- and out-of-phase signals separates these two components [Fig. 2(D)], but the subtraction of the large single-beam bleach introduces significant noise into the second-order grating signal. Drift in the amplitude of the signal can also cause systematic errors in the subtraction. Because interpreting MUPPETS data depends on measuring differences between the first- and second-order correlation functions, eliminating this potential error is critical.

C. Differential Detection

The purpose of this paper is to propose and test differential detection as an alternative to phase modulation. The key insight comes from Eq. (6): changing the roles of a and b is identical to a change in sign of the phase. A detector is placed in each of the two probe beams, and the difference in the normalized signals is taken to yield the differential signal,

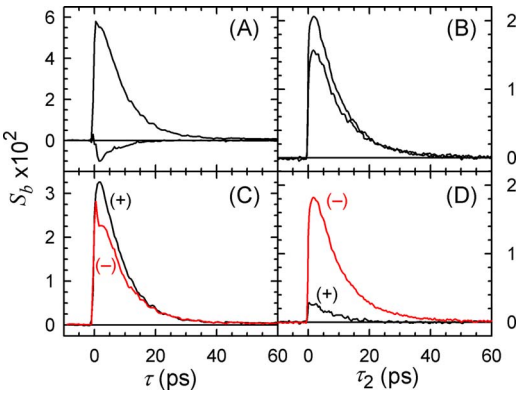

Fig. 2. (Color online) Conventional one-detector heterodyne detection of a first-order (left) and a second-order (right) transient grating. Top row: fractional change in the probe-beam intensity with the phase changed by 180° in (A) a first-order transient grating and (B) a second-order grating. Bottom row: normalized grating signal (black, +) and single-beam bleach (red, −) obtained by addition and subtraction of the signals of opposite phase in (C) a first-order transient grating and (D) a second-order grating. The undesirable single-beam bleach is the same size as the desired grating signal in the first-order grating, but much larger in the second-order grating.

$$S_D = S_b[1a] - S_a[1a]. \tag{11}$$

Equation (8) gives the differential signal as

$$S_D = (-1)^{N-1}\frac{4\pi\omega L\rho}{c}\left(\chi' \sin\Phi \frac{I_{N+1,a}+I_{N+1,b}}{\sqrt{I_{N+1,a}I_{N+1,b}}} + \chi'' \cos\Phi \frac{I_{N+1,a}-I_{N+1,b}}{\sqrt{I_{N+1,a}I_{N+1,b}}}\right)\left(\prod_{n=1}^{N+1}\sigma_n I_n\right)C^{(N)}. \tag{12}$$

As expected, the single-beam bleach is eliminated.

An interesting result is that the relative contributions of the real and imaginary parts of the susceptibility (χ' and χ'', respectively) depend not only on the phase but also on the relative intensities of the two probe beams at the sample. In particular, if the intensities of the two probe beams are equal at the sample,

$$S_D[I_a = I_b] = (-1)^{N-1}\frac{4\pi\omega L\rho}{c}(2\chi' \sin\Phi)\left(\prod_{n=1}^{N+1}\sigma_n I_n\right)C^{(N)}. \tag{13}$$

Only the real part of the susceptibility is measured regardless of phase. For a first-order grating, Ogilvie *et al.* [13] have derived this result and used it in experiments. Equation (13) extends the same idea to gratings of arbitrary order. This configuration is valuable because it is difficult to determine the absolute phase Φ, and thus, it is difficult to cleanly separate the susceptibility into real and imaginary terms. Here, the real part can be isolated by only matching beam intensities and without determining the absolute phase.

In the opposite limit, where the a-probe beam is much stronger than the b-probe beam,

$$S_D[I_a \gg I_b] = (-1)^{N-1}\frac{4\pi\omega L\rho}{c}(\chi'' \cos\Phi + \chi' \sin\Phi)\sqrt{\frac{I_{N+1,a}}{I_{N+1,b}}}\left(\prod_{n=1}^{N+1}\sigma_n I_n\right)C^{(N)}. \tag{14}$$

This result is identical to phase modulating the signal [Eq. (10)]. The potential utility is threefold. First, phase modulation typically involves subtracting scans taken minutes apart, whereas differential detection is done on every individual laser shot. As a result, differential detection is much more effective in eliminating noise and drift from the single-beam-bleach signal. Second, noise in the probe-beam intensity I_{N+1} is cancelled, as shown by the term under the radical. Third, differential detection and phase modulation can be combined to provide increased discrimination against the single-beam bleach or other phase-independent interferences.

In practice, the limit $I_a \gg I_b$ only needs to be strictly enforced, if the contributions of the real and imaginary parts of the susceptibility need to be exactly equal. Any significant mismatch in intensities will make both parts readily detectable. In our experiments, we use $I_a = 10I_b$, which is quite practical and introduces only a 22% reduction in the size of the imaginary part relative to the real part.

The results of differential detection are shown in Fig. 3 and can be compared with standard detection in Fig. 2. The in-phase and out-of-phase signals show good symmetry in both the first-order [Fig. 3(A)] and second-order [Fig. 3(B)] gratings. Upon addition and subtraction, the first-order signal [Fig. 3(C)] shows excellent suppression of the single-beam bleach. The single-beam bleach is also greatly suppressed in the second-order grating [Fig. 3(D)], although some phase-independent signal remains. Some of this signal is due to the first pulse pair acting twice to generate a six-wave-mixing signal. This signal is not well phase matched but is not completely suppressed in the

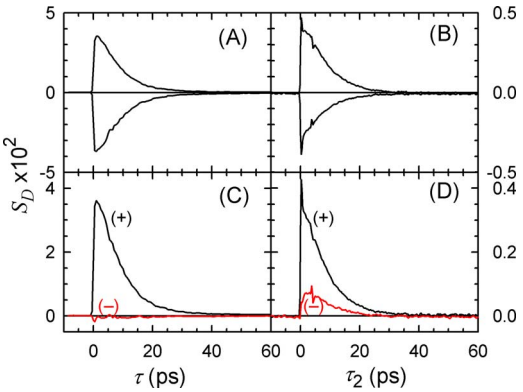

Fig. 3. (Color online) Differential heterodyne detection of a first-order transient grating (left) and a second-order grating (right). Top row: fractional change in the probe-beam intensity with the phase changed by 180° in (A) a first-order transient grating and (B) a second-order grating with $\tau_1 = 0$ ps. Bottom row: normalized differential grating signal (black, +) and single-beam bleach (red, −) obtained by addition and subtraction of the signals of opposite phase in (C) a first-order transient grating and (D) a second-order grating.

current geometry. Phase modulation is still necessary, but the elimination of the large single-beam bleach makes it a more stable process.

The aim of the differential detection was to reduce the noise and drift associated with subtracting a large single-beam bleach. The final signal in the second-order grating is shown with and without differential detection in Fig. 4. The reduction in noise is substantial.

An important consideration in differential detection is that we have assumed that the two probe beams sample the excited region of the sample in exactly the same way. Due to the beam crossing angle, the beams cannot completely overlap over their entire path through the sample. The beam shapes and intensity distributions can also have minor asymmetries, so when the overlap is not complete, one probe beam will sample the excited region more effectively than the other. However, by carefully positioning the sample cell along the beam path, the asymmetries before the crossing will cancel the asymmetries after the crossing. After the beam crossing is optimized through a pinhole, the cell is initially placed with the pinhole position at the center of the cell. The difference signal is adjusted to zero using the variable neutral density filter with the probe beams coming before all excitation pulses. In the six-beam experiments, the probe is placed between the two excitations and small adjustments (a fraction of the 1 mm path length) of the sample position are made to minimize the signal due to beam shape asymmetries. This effect is illustrated in Fig. 5.

4. SUMMARY

This paper has demonstrated a new method of heterodyne detection of transient gratings generated by diffractive optics. This method avoids the conventional picture of distinct probe and local oscillator beams, but rather treats both probe beams equivalently. In particular, both beams are detected, and the differential signal is measured. The intensity changes in the two probe beams prove to be equivalent to heterodyne signals taken with and without a 180° phase shift in the local oscillator. To measure both absorptive and dispersive components of the grating, the probe-beam intensities must be made unequal at the sample, but rematched at the detectors. This method

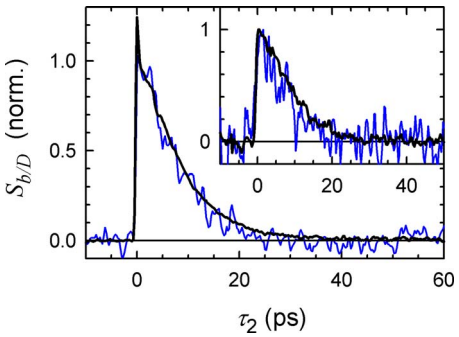

Fig. 4. (Color online) Comparison of MUPPETS signal obtained by using standard detection (blue, noisy curves) and differential heterodyne detection (black, smooth curves) using the same data collection times. Main panel: $\tau_1 = 0$ ps. Inset: $\tau_1 = 10$ ps. The signal-to-noise ratio is improved substantially by using differential detection.

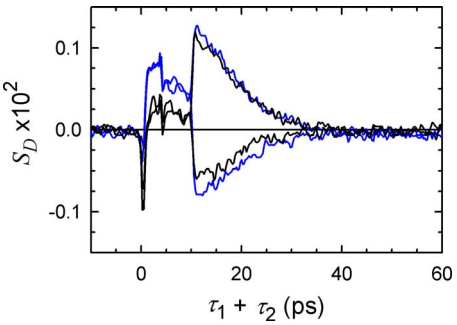

Fig. 5. (Color online) Effect of sample position on differential heterodyne detection: the in- and out-of-phase scans of a second-order-grating signal at $\tau_1 = 10$ ps at two sample positions (black, inner curves and blue, outer curves). A small 0.25 mm movement of the 1 mm thick sample affects the degree to which the single-beam bleach (visible before 10 ps) is suppressed.

eliminates interferences from single-beam-bleach signals and reduces noise from probe-beam intensity fluctuations. Both advantages are useful for standard transient gratings, but are even more important for higher order transient gratings, such as those that are used in MUPPETS experiments.

ACKNOWLEDGMENT

This material is based upon work supported by the National Science Foundation (NSF) under grant CHE-0809306.

REFERENCES

1. A. A. Maznev, K. A. Nelson, and T. A. Rogers, "Optical heterodyne detection of laser-induced gratings," Opt. Lett. **23**, 1319–1321 (1998).
2. G. D. Goodno, G. Dadusc, and R. J. D. Miller, "Ultrafast heterodyne-detected transient-grating spectroscopy using diffractive optics," J. Opt. Soc. Am. B **15**, 1791–1794 (1998).
3. G. D. Goodno and R. J. D. Miller, "Femtosecond heterodyne-detected four-wave-mixing studies of deterministic protein motions. 1. Theory and experimental technique of diffractive optics-based spectroscopy," J. Phys. Chem. A **103**, 10619–10629 (1999).
4. M. Khalil, N. Demirdoven, O. Golonzka, C. J. Fecko, and A. Tokmakoff, "A phase-sensitive detection method using diffractive optics for polarization-selective femtosecond Raman spectroscopy," J. Phys. Chem. A **104**, 5711–5715 (2000).
5. Q.-H. Xu, Y.-Z. Ma, and G. R. Fleming, "Heterodyne detected transient grating spectroscopy in resonant and nonresonant systems using a simplified diffractive optics method," Chem. Phys. Lett. **338**, 254–262 (2001).
6. K. J. Kubarych, C. J. Milne, S. Lin, and R. J. D. Miller, "Diffractive optics implementation of time- and frequency-domain heterodyne-detected six-wave mixing," Appl. Phys. B **74**, S107–S112 (2002).
7. M. J. Ammend and D. A. Blank, "Passive optical interferometer without spatial overlap between the local oscillator and signal generation," Opt. Lett. **34**, 548–550 (2009).
8. E. van Veldhoven, C. Khurmi, X. Zhang, and M. A. Berg, "Time-resolved optical spectroscopy with multiple population dimensions: a general method of resolving dynamic heterogeneity," ChemPhysChem **8**, 1761–1765 (2007).
9. C. Khurmi and M. A. Berg, "Analyzing nonexponential kinetics with multiple population-period transient

spectroscopy (MUPPETS)," J. Phys. Chem. A **112**, 3364–3375 (2008).
10. C. Khurmi and M. A. Berg, "Parallels between multiple population-period transient spectroscopy (MUPPETS) and multidimensional coherence spectroscopies," J. Chem. Phys. **129**, 064504 (2008).
11. M. A. Berg has prepared a manuscript to be called "Hilbert-space treatment of incoherent, time-resolved spectroscopy. I. Formalism, a tensorial classification of high-order orientational gratings and generalized MUPPETS 'echoes' ."
12. M. A. Berg has prepared a manuscript to be called "Hilbert-space treatment of incoherent, time-resolved spectroscopy. II. Pathway description of optical MUPPETS."
13. J. P. Ogilvie, M. Plazanet, G. Dadusc, and R. J. D. Miller, "Dynamics of ligand escape in myoglobin: Q-band transient absorption and four-wave mixing studies," J. Phys. Chem. B **106**, 10460–10467 (2002).
14. G. Giraud, C. M. Gordon, I. R. Dunkin, and K. Wynne, "The effects of anion and cation substitution on the ultrafast solvent dynamics of ionic liquids: a time-resolved optical Kerr-effect spectroscopic study," J. Chem. Phys. **119**, 464–477 (2003).
15. E. C. Fulmer, P. Mukherjee, A. T. Krummel, and M. T. Zanni, "A pulse sequence for directly measuring the anharmonicities of coupled vibrations: two-quantum two-dimensional infrared spectroscopy," J. Chem. Phys. **120**, 8067–8078 (2004).
16. J. J. Loparo, S. T. Roberts, and A. Tokmakoff, "Multidimensional infrared spectroscopy of water. I. Vibrational dynamics in two-dimensional IR line shapes," J. Chem. Phys. **125**, 194521 (2006).